Vaccine 37 (2019) 6857–6867

Contents lists available at ScienceDirect

Vaccine

journal homepage: www.elsevier.com/locate/vaccine

Influenza A and B virus-like particles produced in mammalian cells are highly immunogenic and induce functional antibodies

Sophie Buffin [a,*], Isabelle Peubez [a], Fabienne Barrière [a], Marie-Claire Nicolaï [a], Tenekua Tapia [b], Vipra Dhir [b], Eric Forma [a], Nicolas Sève [a], Isabelle Legastelois [a]

[a] Sanofi Pasteur, Research and Development, Marcy L'Etoile, France
[b] Sanofi Pasteur, VaxDesign Campus, 2501 Discovery Drive Suite 300, Orlando, FL 32826, USA

ARTICLE INFO

Article history:
Received 23 May 2019
Received in revised form 13 September 2019
Accepted 18 September 2019
Available online 4 October 2019

Keywords:
Influenza
Virus-like particle
Vaccine
Transient transfection
Neuraminidase inhibition

ABSTRACT

Influenza virus-like particles (VLPs) represent an attractive alternative to traditional influenza vaccine formulations. Influenza VLPs mimic the natural virus while lacking the genetic material, are easily recognized by the immune system, and are considered safe. The use of a mammalian cell platform offers many advantages for VLP production, such as flexibility and the same glycosylation patterns as a human virus. In this study, the influenza VLPs containing hemagglutinin (HA), neuraminidase (NA) and matrix M1 proteins were expressed in CHO-K1, Vero or 293 T cell lines using transient transfection. After production in 3L bioreactor and purification, extensive characterization was performed on two batches of VLPs produced in 293 T, the best cell line for VLP expression; one batch expressed the HA and NA genes from A/Hong Kong/4801/2014 (H3N2) strain and the other, HA and NA genes from B/Phuket/3073/2013. Characterizations provided evidence that mammalian VLPs closely emulate the exterior of authentic virus particles in terms of both antigen presentation and biological properties. The two VLPs produced contained more NA proteins on their surface with a HA:NA ratio around 1:1 than influenza viruses which present a HA:NA ratio of around 4:1. Immunogenicity studies in BALB/c mice demonstrated that the VLPs, administered intra-muscularly, were highly immunogenic at low doses, with the induction of functional antibodies against HA and NA. Immunogenicity was also shown in a human *in vitro* model (MIMIC® system). In conclusion, we believe that influenza vaccines made of VLPs produced in mammalian cell lines, constitute a potential alternative to the classical influenza vaccines.

1. Introduction

Influenza viruses are negative stranded RNA viruses of the *Orthomyxoviridae* family. Three types of influenza virus, A, B and C, are capable of infecting humans, with influenza A and B the most common circulating types. Hemagglutinin (HA) and neuraminidase (NA) are key surface glycoproteins of influenza viruses. HA, a major antigen, binds to the sialic acid residues on the cell surface, allowing viral entry into the cell. NA is less abundant on the viral surface than HA, the commonly observed HA:NA ratio being 4:1 [1]. Its enzymatic activity is important for cleaving sialic acid, hence facilitating virus release from the surface of the infected cell. NA activity also allows influenza to penetrate the mucus by a mechanism involving sialic acid cleavage but remains to be fully established [2]. Both proteins lead to antibody responses upon infection: HA-specific antibodies confer protective immunity [3], while NA-specific antibodies reduce the severity of the disease by restricting viral replication.

The World Health Organization (WHO) estimates that between 500 million and 1 billion people are affected by influenza every year; hundreds of thousands of those cases result in fatalities [4]. Vaccination is considered the most effective method of protection from the disease. Every year the WHO releases recommendations for the strains to be included in the influenza vaccine based on an epidemiological analysis of the circulating strains: two influenza type A strains (A [H1N1] subtype and A [H3N2] subtype) and two influenza type B strains (B/Yamagata and B/Victoria lineages). Classical influenza vaccines are either inactivated (IIV) or live-attenuated influenza vaccines (LAIV), both requiring seasonal administration. Currently, influenza vaccine production relies on the use of embryonated chicken eggs to culture the virus. Although

* Corresponding author at: Sanofi Pasteur, 1541 Avenue Marcel Mérieux, 69280 Marcy L'Etoile, France.
E-mail addresses: sophie.buffin@sanofi.com (S. Buffin), isabelle.peubez@sanofi.com (I. Peubez), fabienne.barriere@sanofi.com (F. Barrière), marie-claire.nicolai@sanofi.com (M.-C. Nicolaï), tenekua.tapia@sanofi.com (T. Tapia), vipra.dhir@sanofi.com (V. Dhir), eric.forma@sanofi.com (E. Forma), nicolas.seve@sanofi.com (N. Sève), isabelle.legastelois@sanofi.com (I. Legastelois).

https://doi.org/10.1016/j.vaccine.2019.09.057
0264-410X/

this process is well controlled and efficient, it carries drawbacks that have been described elsewhere [5,6].

Two new products, based on cell-based production methods, have been introduced and FDA-approved in recent years: a cell culture-derived IIV produced on Madin–Darby canine kidney (MDCK) cells approved in 2012 [7], and a recombinant influenza vaccine containing the influenza HA protein, expressed in an insect cell line, approved in 2014 [8].

Another promising alternative to traditional influenza vaccine formulations is virus-like particles (VLPs). VLPs mimic the natural virus while lacking the viral genetic material. They are easily recognized by the immune system, and are considered to be safe [9,10]. The VLP production process is viral free and does not require any high level containment facilities or complex inactivation steps. In contrast to the currently available influenza vaccines which contain antigen fragments or soluble proteins, influenza VLPs are particulates by nature and display intact and biochemically active viral antigens on their surface.

In the literature, influenza VLPs are composed of one or different combinations of the viral surface glycoproteins, HA, NA, and the structural influenza protein matrix 1 (M1), with or without the matrix-2 (M2) ion channel [11,12]. Influenza VLPs have been produced in various expression systems; mammalian, insect and plant cells [13–15] and in Eri silkworm pupae [16].

In this study, we chose to produce influenza VLPs in mammalian cell lines using transient transfection [17]. Mammalian cell culture systems offer several advantages including the flexibility and consistency during process manufacturing. Additionally, they allow the recovery of glycosylated proteins with lipid membrane compositions that closely resemble those of the virus host. In the literature, VLPs are often produced after stable transfection of viral genes into cultures of mammalian cells, such as Vero [12] or 293 cells [15,18,19]. In contrast, in this study, transient gene expression (TGE) was chosen over stable transfection to reduce the production time. After transfection, plasmid DNA molecules remain in the cells without being integrated into the genome, and are eventually lost over time and cell division. The accelerated development of gene therapy, personalized medicine and new requirements in the vaccine field are driving an increasing interest in scaling-up TGE, including for the production of VLPs [17,20].

In this work, influenza H1N1 VLPs constituted of HA, NA and M1 were expressed in CHO-K1, Vero and 293 T cell lines by transient transfection. After purification, extensive characterization was performed on two batches of VLPs produced into 293 T, the most productive one, expressing HA and NA genes from either the A/Hong Kong/4801/2014 (H3N2) strain or B/Phuket/3073/2013 strain. The M1 protein from A/California/07/2009 (H1N1) was chosen for all VLPs expressing the HA and NA from type A or B. This pandemic H1N1 M1 protein was reported to induce very efficient budding at the plasma membrane, unlike other influenza virus M1 proteins [21]. VLP immunogenicity was studied in BALB/c mice and in a human *in vitro* model.

2. Materials and methods

2.1. Influenza genes and expression constructs

The HA, NA and M1 protein sequences of the WHO recommended influenza strains for the 2016/2017 season were obtained from GISAID Epiflu or from NCBI GenBank databases (Table 1). All plasmids were designed and constructed by Oxford Genetics (supplementary materials). All influenza genes except M1 were codon optimized for expression in mammalian cells and cloned into an expression vector, under the cytomegalovirus promoter fused with the elongation factor-1 alpha promoter. All vectors contained the simian virus 40 polyA, except the M1 vector which contained the rabbit beta globin polyA. The M1 plasmid included the KsBcl-2 gene which corresponds to an anti-apoptotic protein designed to improve cell viability post-transfection [22]. The vector containing the M1 gene from A/California/07/2009 (H1N1) was used for all the VLPs expressing the HA and NA from type A or B on their surface.

Table 1
List of Influenza proteins included in the plasmids that were used in the VLP productions.

Type of protein	Strains	GenBank or GISAID Epiflu accession number
M1	A/California/07/2009 (H1N1)	FJ966975
HA	A/California/07/2009 (H1N1)	FJ966974
HA	A/Hong Kong/4801/2014 (H3N2)	EPI578430
NA	A/California/07/2009 (H1N1)	CY121682
NA	A/Hong Kong/4801/2014 (H3N2)	EPI578429
HA	B/Brisbane/60/2008	KX058884.1
HA	B/Phuket/3073/2013	EPI544264
NA	B/Brisbane/60/2008	CY073894.1
NA	B/Phuket/3073/2013	EPI544263

The HA and NA protein sequences of each strain were chosen according to the WHO recommendations for Influenza vaccine formulations for the 2016–2017 season.

2.2. VLP production in various mammalian cells (small scale)

Chinese hamster ovary CHO-K1 cells were cultured in suspension, in the serum-free EX-CELL CDCHO FUSION media (Sigma Aldrich) at 37 °C, 120 rpm and 5% CO_2. Ten million cells were nucleofected in the V Buffer (Lonza) with the AMAXA nucleofector (Lonza) and 15μg of the 3 plasmids (5μg of each). The supernatant containing VLPs were harvested 6 days after the transfection.

Adherent Vero cells were cultured in the serum-free VP-SFM media (Gibco) at 37 °C and 5% CO_2. The cells were plated in flasks of 175 cm^2 and transfected at ~ 80% of cell confluence with 90 μg of the 3 plasmids (30 μg each) mixed with Lipofectamine 3000 reagent (ThermoFisher), according to supplier's instructions. The supernatant was harvested 6 days after the transfection.

293 T cells were cultured in suspension in the serum-free FreeStyle F17 Expression (ThermoFisher) media supplemented with 6 mM of L-glutamine and 0.08% of pluronic acid at 37 °C, 120 rpm and 5% CO_2. Fifty million cells were adjusted to 2.10^6 cells/mL and transfected with 100μg of the 3 plasmids (33.3μg each) mixed with PEIpro reagent (Polyplus). The temperature was reduced to 33 °C at 1 day post-transfection. The supernatant was harvested 4 days after transfection.

The supernatants from 293 T, CHO-K1 and Vero cells were clarified by centrifugation and concentrated on Vivaspin column (Sartorius) using a100 kDa cutoff. For analysis by cryo-transmission electron microscopy (cryo-TEM), the VLPs were semi-purified on a sucrose cushion. Briefly, VLP concentrated supernatants were loaded into ultracentrifuge tubes and underlayed with 30% of sucrose cushion. Ultracentrifugation was performed at 110,000 g, 10 °C for 2 h. Supernatants were discarded and VLP pellets were re-suspended overnight at 4 °C in phosphate buffered saline. The sucrose contaminant was removed with Zeba chromatography column (ThermoFisher). This step allowed VLP sample concentration of up to 20–100 folds.

2.3. VLP production in 3L disposable bioreactor and purification

Mobius® CellReady 3L-bioreactors (Merck Millipore) were used to produce VLPs in suspension 293 T cells under controlled and monitored conditions (25% Dissolved Oxygen, 7.2 pH, 37 °C, 230 rpm), with the same transfection conditions as those used for the small-scale production (Fig. 1). Harvest clarification was

performed by centrifugation followed by filtration. Protein impurities were removed through a Captocore chromatography resin. Purified column fractions were pooled, concentrated by tangential flow filtration and diafiltrated. To decrease cell DNA concentration, two Benzonase treatments were performed: after harvest clarification and before diafiltration.

2.4. Western blot

Western blot analysis was performed to detect HA, NA and M1 proteins from the A/California/07/2009 (H1N1) strain. The VLP samples were mixed with 0.1 M DTT (SIGMA) and NuPAGE LDS sample buffer (ThermoFisher), heated for 10 min at 95 °C and separated on a 4–12% Bis-Tris SDS-PAGE (ThermoFisher). After gel-transfer and saturation, the blots were incubated with a rabbit polyclonal antibody against H1N1 influenza A virus NA (RD System), a polyclonal sheep antibody against H1N1 M1 (ThermoFisher), or a polyclonal rabbit antibody against the HA from A/California/07/2009 (H1N1) (produced in-house) for 1 h. Blots were then incubated with a secondary sheep anti-rabbit or anti-sheep antibody conjugated to IRDye 800 (Rockland) for 1 h. The membranes were visualized using Odyssey Infrared Imaging System (LICOR, Bioscience). Influenza A/California/07/2009 (H1N1) inactivated virus (NIBSC code 09/174) was loaded as a positive control.

2.5. Haemagglutination assay

A standard haemagglutination assay (HAU, haemagglutination unit) using a 0.5% suspension of turkey red blood cells (Sanofi Pasteur) was carried out as previously described [23]. Three independent determinations were performed for each VLP sample.

2.6. Neuraminidase enzymatic assay

To determine functional NA enzyme activity, a fluorescence-based NA assay (NA-Fluor from ThermoFisher) was used with 4-methylumbelliferone-N-acetyl neuraminic acid as a substrate, according to supplier's instructions. Commercial recombinant NA (ThermoFisher) was used as a positive control. A standard curve to determine a relative fluorescence unit value within the linear range of fluorescence detection was generated using 12 concentrations of 4-methylumbelliferone sodium salt (Sigma Aldrich) from 0 to 100 μM. Fluorescence was read on the Varioskan reader (ThermoScientific) after one hour at 37 °C. NA activity titers were expressed in μM/h. Three independent determinations were performed for each VLP sample.

2.7. Single radial immunodiffusion (SRID)

The amount of HA protein was assessed by SRID assay, using the reference method recommended by the regulatory authorities [24] and currently used for quantifying HA protein in vaccine batches. SRID reference sheep sera reagents from NIBSC, code 16/182 and 15/150 were used to quantify A/Hong Kong/4801/2014 (H3N2) and B/Phuket/3073/2013 strains, respectively; the influenza antigen reagent codes were 15/230 for A/Hong Kong/4801/2014 (H3N2) and 16/158 for B/Phuket/3073/2013. Three independent determinations were performed for each VLP sample.

2.8. Total protein quantification

The total protein content of each purified sample was measured using a classical Bradford assay (Biorad). Bovine serum albumin was used to create a standard curve and the samples were read at 595 nm on the Varioskan reader (ThermoScientific). Three independent determinations were performed for each VLP sample.

2.9. DNA content

DNA contaminant was measured by Qubit dsDNA high sensitivity kit (ThermoFisher) with Qubit fluorometer according to supplier's instructions. Three independent determinations were performed for each VLP sample.

2.10. SDS-PAGE for densitometry analysis

Analyses were carried out on a 4–12% (w/v) SDS PAGE (XT Criterion Bis Tris gels, Bio-Rad) using MOPS (Bio-Rad) as running buffer. Prior to analysis, VLP samples were concentrated on Amicon® Ultra Centrifugal Filters 0.5 mL–3 K. Total protein (2 μg) was denaturated by addition of 2X Laemmli Sample Buffer (Bio-Rad). For samples under reducing conditions, DTT was added at a final concentration of 25 mM. For deglycosylated samples, total protein (2 μg) was deglycosylated with PNGase F according to the N-Glycanase kit protocol (PROzyme®). Samples were heated to 100 °C for 5 min and then loaded into the wells. Gels were stained using GelCodeTM Blue Stain Reagent (ThermoScientific). The analysis was performed in triplicate. Densitometry analysis of SDS-PAGE was performed using GS900 densitometer (BioRad) and Image LabTM software.

2.11. Protein quantification by mass spectrometry

VLP samples were submitted to trypsin (Promega) digestion after denaturation with sodium deoxycholate 2% (w/v). AQUA® peptide standards [25,26] were added before digestion. After desalting (Oasis® HLB 1 cc Extraction Cartridges, WATERS), sample peptide mixtures were analyzed on a triple quad mass spectrometer (TQ6490 Agilent) coupled to liquid chromatography (ULPC 1290 Agilent), and data were processed with the open source software Skyline [27]. Absolute quantification was obtained from the heavy/light ratio multiplied by the amount of standard spiked into

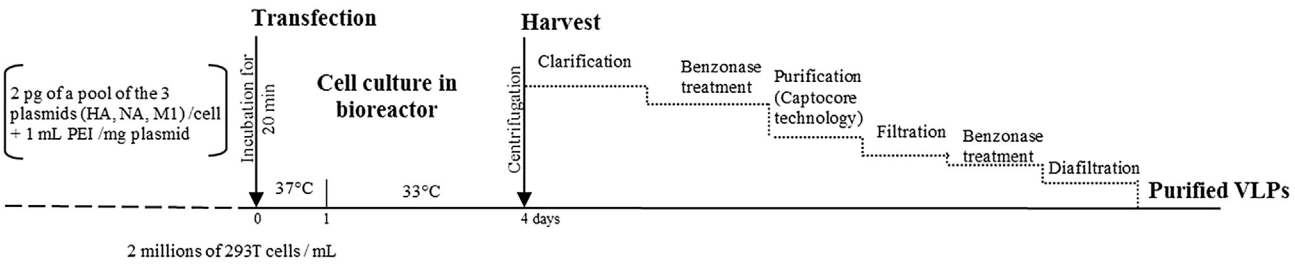

Fig. 1. Scheduling of the production process of influenza VLPs produced in 293 T cells at large scale.

the sample. The analysis was performed in triplicate and for each protein, means, standard deviation values were calculated.

2.12. Particle size by nanoparticle tracking analysis (NTA)

NTA measurements rely on light scattering and Brownian motion technology to determine the size distribution and concentration of particles in VLP samples. The analysis was performed using a NanoSight NS300 instrument from Malvern, according to the supplier's guide [28]. Each sample was analyzed once, and live monitoring NTA acquisition was carried out using a syringe loading system. For sample validation, a minimum of 1000 quantified tracks were obtained for three independent videos of 60 s acquisition. Data were processed with Nanosight NTA 3.1 software (Malvern).

2.13. Electron microscopy

2.13.1. Ultrastructural analysis of the 293 T cells by transmission electron microscopy (TEM)

This analysis was performed by IBiSA, University of Tours as previously described [29]. 293 T cell sections were observed using a JEOL 1011 transmission electron microscope.

2.13.2. Analysis of VLPs by cryo-transmission electron microscopy (cryo-TEM)

This analysis was performed by CBMN, UMR 5248, University of Bordeaux. A 4.2 µl sample of viral particles was deposited onto a lacey carbon copper grid submitted to glow discharge. The supernatant of the non-transfected cells was used as a negative control. After removing excess solution with filter paper, the grid was rapidly plunged into a liquid ethane bath and cooled with liquid nitrogen by using an EM GP instrument (Leica). Samples were maintained at a temperature of approximately −170 °C by using a cryo-holder (Gatan), and observed with a FEI Tecnai F20 electron microscope operating at 200 kV. Images were acquired by using a digital 2 k × 2 k USC1000 camera (GATAN).

2.14. Immunization of mice

Groups of ten 8-week-old female BALB/c mice received two IM injections under light anesthesia with isoflurane three weeks apart. Two doses of 1.2 or 0.4 µg of H3N2 VLPs or B/Phuket VLPs diluted in phosphate-buffered saline (PBS) were administered to each mouse. The quantity injected was based on HA content measured by SRID assay. Influenza-naïve control mice received injections of VLP buffer used in the final step of the purification process (composed of Tris buffer, NaCl, Sucrose, Mannitol and Poloxamer 188). Blood samples were collected under anesthesia three weeks after the second injection (day 42). The study was approved by the Sanofi Pasteur internal animal care committee and was performed in accordance with EU directive 2010/63/EU for animal experimentation.

2.15. Serology

Antibody responses were measured using a standard hemagglutination inhibition (HI) assay and enzyme-linked immunosorbent assay (ELISA) dosage of specific antibodies in the serum samples (IgG), as described previously [30]. The presence of HI antibodies against the various influenza strains was assessed using chicken red blood cells (cRBCs). HI assays were performed on individual serum samples treated with Receptor Destroying Enzyme, cRBCs and 6- (1-tosylamido-2-phenyl) ethyl chloromethyl ketone (TPCK) trypsin to totally remove hemagglutination inhibitors present in murine sera [31]. The HI assay was performed against live viruses (H3N2 or B/Phuket) produced in eggs. ELISA assays were performed after an overnight coating at +4 °C with 100 ng/well of the corresponding inactivated virus (Vaxigrip, Sanofi Pasteur). Antibody titers were calculated using the Soft Max Pro software (version 6.4).

NA inhibition (NI) antibody was measured by Enzyme-Linked Lectin Assay (ELLA) described by Couzens et al. [32], except that VLPs expressing NA and M1 only, obtained as previously described, were used instead of recombinant NA. Briefly, serial dilutions of heat-inactivated sera were incubated at 37 °C overnight on fetuin-coated plates with a fixed amount of NA VLP. This amount of NA was determined as the dilution that gave approximately 90% of the maximum signal. The reciprocal of the highest serum dilution that resulted in ≥50% inhibition of NA VLP activity was designated as the NI antibody titer.

2.16. In vitro MIMIC® system

2.16.1. Donors

Peripheral blood mononuclear cells (PBMCs) from 10 healthy human donors were collected. Informed consent was obtained from each subject prior to enrolment. After processing, the PBMCs were cryopreserved and stored in vapor phase liquid nitrogen until needed.

2.16.2. MIMIC® system

A MIMIC® transwell peripheral tissue equivalent module was used to generate antigen presenting cells (APCs) as previously described [33]. Briefly, pre-vaccination donor PBMCs were applied to transwells containing confluent endothelial cells (EA.hy 926, ATCC) in a 24-well plate followed by stimulation for 24 h with 10 ng of A/Hong Kong inactivated vaccine (Vaxigrip, Sanofi Pasteur) or 10 ng of H3N2 VLPs or nothing. Culture supernatants were collected for detection of total and functional anti-HA IgG antibodies to H3N2 strain using multiplexed bead-based ELISA performed on a Luminex platform (Antibody Forensics) and surface-assisted HA inhibition assay (SA-HAI), respectively as previously described [34,35].

2.17. Statistical analysis

Statistical analyses were conducted using Prism 6 (GraphPad). Statistical differences between means of the two doses of VLPs for HI titers, NI titers and IgG were analyzed using Student *t*-test. P values < 0.05 were considered statistically significant.

3. Results

3.1. Screening of various mammalian cell types for the production of influenza A/California/07/2009 (H1N1) VLP

First, we tried to produce A/California/07/2009 (H1N1) VLPs in various mammalian cell types. Optimized vectors were used for the transient transfection of the H1N1 HA, NA and M1 influenza genes to achieve the best possible expression of VLPs. The best of the three HA-NA-M1 plasmid combinations was transiently transfected into the CHO-K1, Vero and 293 T cells in parallel, using an optimized transfection protocol for each cell line. M1, HA and NA were detected in the CHO-K1 supernatant (concentrated x10). None of these proteins were detected in the Vero supernatant (concentrated x60). However, all three proteins were detected in the 293 T cell supernatant without the need to concentrate the supernatant (Table 2 and Fig. 2A). Functional HA and NA expression was observed in 293 T and CHO-K1 VLPs. The highest values were obtained for the 293 T cell line reaching a titre of 638 HAU

Table 2
Protein detection and HA and NA activity from A/California/07/2009 (H1N1) measurement in the cell supernatant.

Cells	CHO-K1	Vero	293 T
HAU for 100.10^6 cells	200	<1	638
NA activity (μM/h) for 100.10^6 cells	320	2	2660
HA, NA, M1 protein detection by Western Blot	+/− (×10)	−(×60)	++(×1)

Not detected (−)/very low detection (+/−)/well-detection (++)/(concentration factor of the supernatant).

and a NA activity of 2660 μM/h for 100 million cells. Unlike CHO-K1 and 293 T cell supernatants, Vero supernatant presented no HAU titer and very low NA activity (Table 2).

The VLPs obtained from the three systems were observed by cryo-TEM. Vero VLPs were less abundant on the grids than CHO-K1 or 293 T cell VLPs. The three cell lines produced particles of around 100 nm presenting a lipid membrane. The particles were decorated with protein spikes, which closely resembled HA and NA spikes on the egg-produced virus (Fig. 2B). The 293 T and Vero VLPs contained a higher density of HA and NA spikes than the CHO-K1 VLPs. Of note, Vero cell supernatant presented no HAU titer and very low NA activity, linked to a poor production yield of total VLPs, but individual VLPs observed by cryo-TEM produced in this system seemed to express high amounts of HA and NA spikes. The non-transfected controls for the three cell lines contained only some protein aggregates and lipid vesicles without any spikes (data not shown). Overall, the 293 T cell line gave the best results in terms of VLP yield and morphology so this cell line was chosen to express different influenza strains.

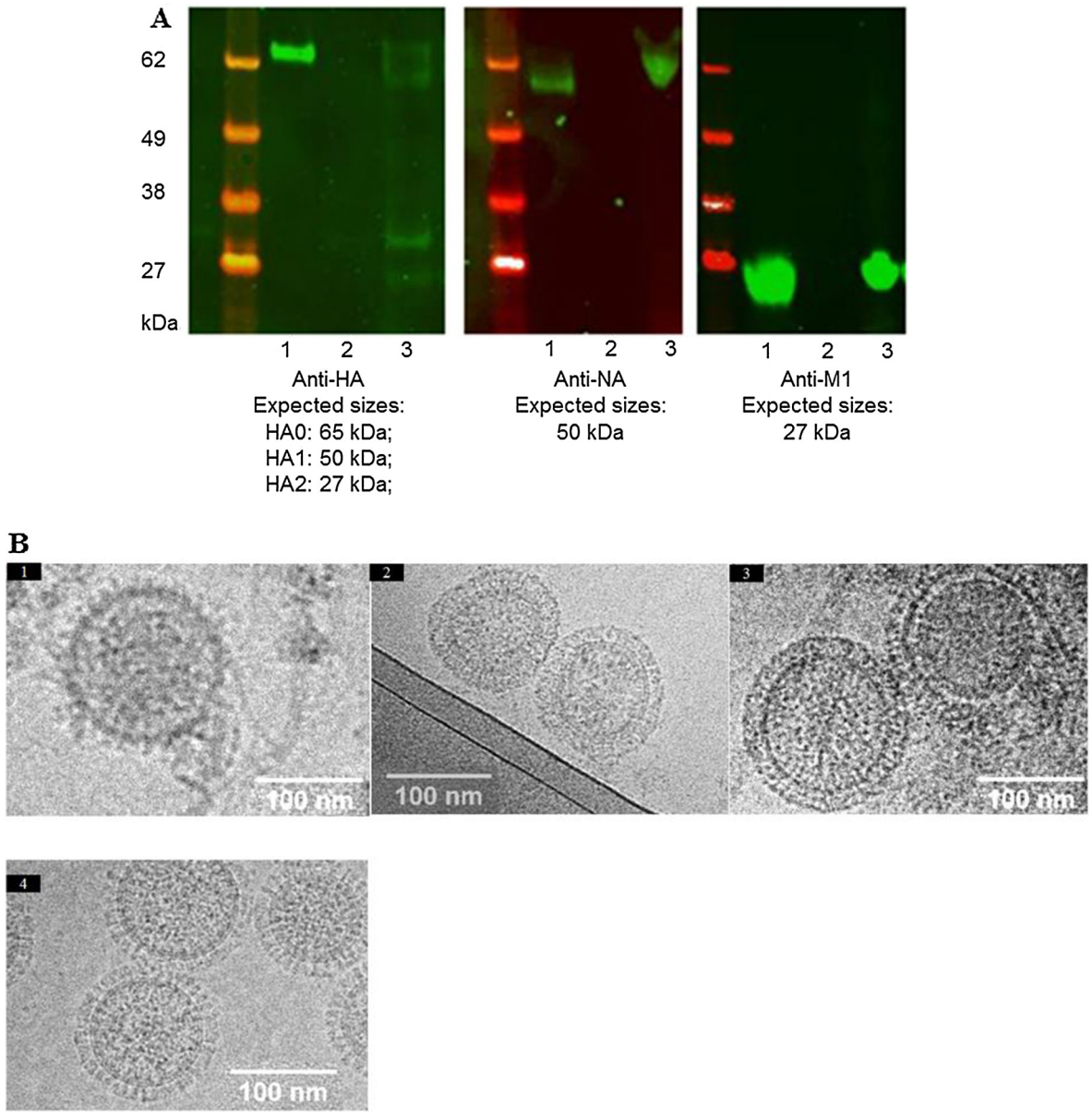

Fig. 2. Screening mammalian cell types for the influenza A/California/07/2009 (H1N1) VLP production (A) HA, NA, M1 protein detection by Western Blot with specific antibodies in the supernatant of the 293 T cells expressing VLPs (1) NIBSC influenza H1N1 antigen as positive control, (2) supernatant of 293 T cell as negative control, (3) supernatant of 293 T cell expressed influenza VLPs; (B) VLPs expressed in CHO-K1 cells (1), Vero cells (2), 293 T cells (3) and A/H3N2 influenza virus as positive control (4) were observed by Cryo-TEM performed by CBMN, UMR 5248, University of Bordeaux.

3.2. Production of influenza VLPs from different influenza strains in 293 T cells in a disposable 3L bioreactor

To assess the versatility of the process set-up, four different VLPs were expressed in 293 T cells in 3L bioreactors, including two A and two B strains as recommended by the WHO for the 2016/2017 season: A/California/07/2009 (H1N1), A/Hong Kong/4801/2014 (H3N2), B/Brisbane/60/2008 and B/Phuket/3073/2013. With the exception of the HA and NA sequences the design of the HA, NA and M1 plasmids used to transfect the 293 T cells was identical for all four strains.

Cell count and cell viability were monitored daily (Fig. 3A). Cell concentration was between 2 and 4.10^6 cells/mL at the end of the culture corresponding to four days post-transfection. Cell viability was around 70% for the four types of VLPs after transfection. The decrease in cell viability was probably due to a toxic effect of the PEIpro reagent, and the influenza protein expression despite the expression of an anti-apoptotic protein (KsBCL2) produced from the M1 plasmid. Large differences in HAU and NA activity titers were observed between the four strains even though they contained a homologous M1 (Fig. 3B). Low HAU and NA activity titers were obtained for the H1N1 VLP batch, (39 HAU/mL, 38 μM/h of NA activity). The highest HAU and NA activity titers were observed with the B/Phuket VLPs (5,011 HAU/mL, 2, 691 μM/h of NA activity). The H3N2 VLPs showed similar NA activity compared to the B/Phuket VLPs, but the HAU titer was lower (631 HAU/mL, 2,884 μM/h of NA activity). The B/Brisbane VLPs presented a similar HAU titer compared to the H3N2 VLPs but a low NA activity titer equivalent to the H1N1 VLPs (223 HAU/mL, 20 μM/h of NA activity) (Fig. 3B). Similar HAU and NA activity titers were observed between small scale in erlen and large scale in 3L bioreactor (data not shown). The 293 T cells were observed by TEM at D4 after transfection (Fig. 3C). The budding of VLPs from cells was shown for all the strains. However, for the H1N1 and B/Brisbane strains that presented low NA activities, the VLPs appeared to remain attached to the cell membrane with granules visible around the aggregated VLPs, especially for the H1N1 strain. Purification was successful only for the H3N2 and B/Phuket VLPs, and not for the H1N1

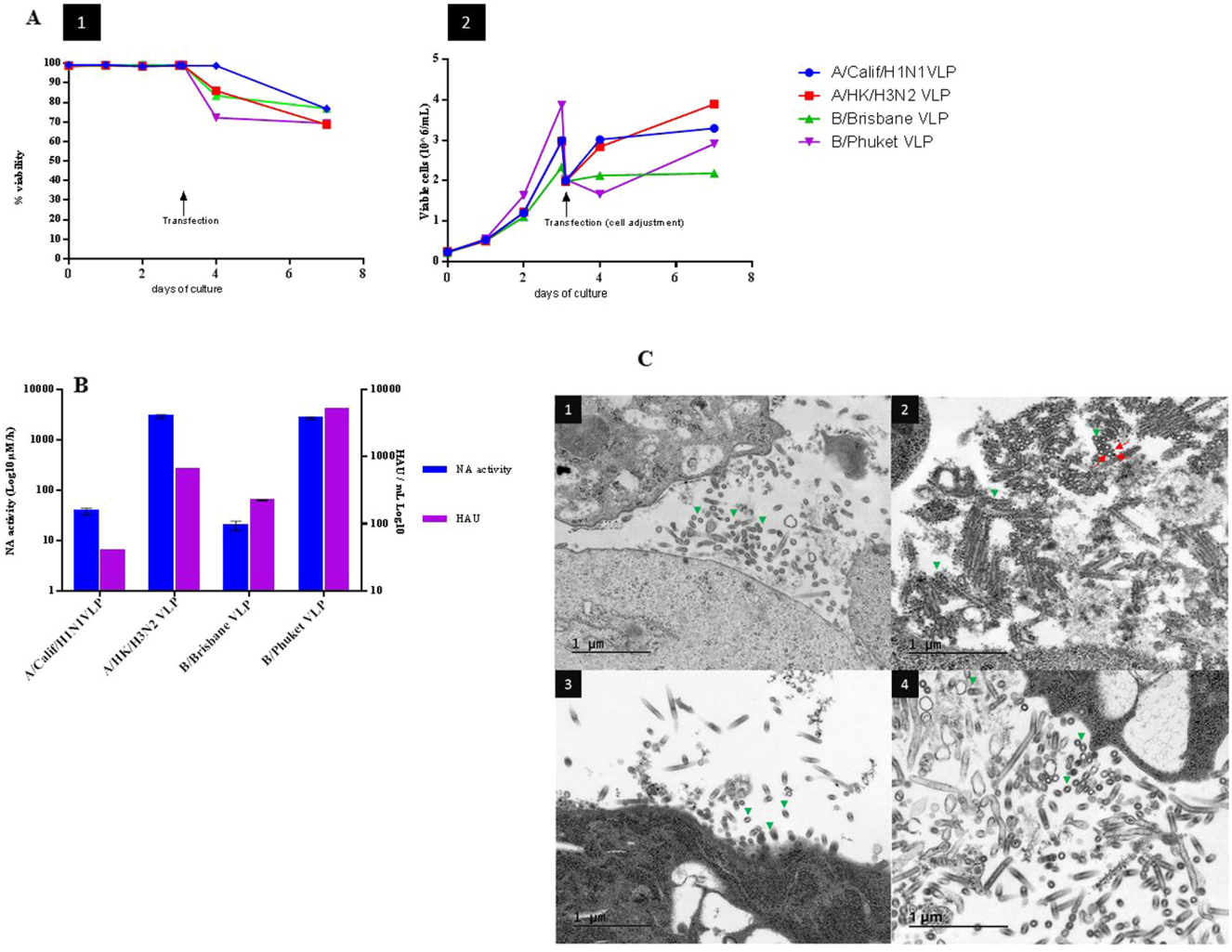

Fig. 3. Production of influenza VLP from different strains in 293 T cells in disposable 3L-Bioreactor. The results of one representative experiment for each VLP batch are presented. (A) Time course of cell viability (1) and viable cell growth (2) during VLPs production (B) HAU and NA activities measured in the clarified cell supernatant 4 days after transfection. Data displayed as the mean ± standard deviation (C) TEM on the 293 T cells producing VLPs at D4 after transfection. Ultrathin sections of the cells showed the presence of numerous VLPs (green arrow) budding from the cell membrane (1) H3N2 VLP, (2) H1N1 VLP with granules visible around the aggregated VLPs (red arrow), (3) B/Phuket VLP, (4) B/Brisbane VLP. TEM analyses performed by IBiSA, University of Tours.

Table 3
Monitoring of the purification process for the B/Phuket VLPs.

Purification Step	Volume (mL)	DNA (ng/mL)	DNA removal %	Total protein (μg/mL)	Protein removal %	NA activity (μM/h)	NA activity recovery %
Centrifuged harvest	1721	2960	0	320	0	2691	100
Clarified harvest	1673	2280	23	153	54	752	27
After benzonase	1677	610	80	138	58	752	27
After purification	2037	288	91	17	94	574	25
Final product	49	56	97.8	39	99.7	16,627	17

Table 4
Summary of the panel of characterizations performed on the purified influenza H3N2 and B/Phuket VLPs.

	Purified H3N2 VLP					Purified B/Phuket VLP				
	SRID (μg/mL)	Mass Spectrometry (μg/mL)	HA activity HAU/mL	NA activity by MUNANA (μM/h)	Particle count and size by NTA	SRID (μg/mL)	Mass Spectrometry (μg/mL)	HA activity HAU/mL	NA activity by MUNANA (μM/h)	Particle count and size by NTA
HA	40 ± 7.9 1.35 mg/L of culture	14 ± 2.3	25,539	N/A	3.67×10^{11} part/mL Mode 97 nm/	12 ± 1.4 348 μg/L of culture	12 ± 0.9	102,157	N/A	2.56×10^{11} part/mL Mode 109 nm/
NA	N/A	19 ± 1.3	N/A	35,325	Median	N/A	11 ± 0.6	N/A	16,627	Median
M1	N/A	7 ± 1.2	N/A	N/A	118.5 nm Polydisperse (Span* = 0.87)	N/A	6 ± 0.6	N/A	N/A	117.5 nm Polydisperse (Span* = 0.79)

N/A: non-applicable.
* Span: polydispersity index; <0.1 monodisperse >0.1 polydisperse.

and B/Brisbane VLPs, despite several attempts, probably due to the low amount of VLPs produced in the batches.

3.3. Characterization of purified influenza VLPs

M1 protein expression, NA activity, DNA and total protein contents were monitored throughout the purification process (supplementary material). The results for the B/Phuket strain (as a representative example) are presented in Table 3. The purification process eliminated more than 97% of the DNA content, and more than 99% of the total cellular proteins. In addition, 17% of NA activity was recovered after the final purification step for the B/Phuket strain. Purified H3N2 and B/Phuket VLPs were extensively characterized (Table 4; Fig. 4). HA concentrations, assessed by SRID, were 1.35 mg and 348 μg per liter of culture for H3N2 and B/Phuket VLPs respectively, which is consistent with high HAU titers monitored (25,539 and 102,157, HAU/mL respectively). Mass spectrometry assessments showed that NA content was equivalent to HA content for the B/Phuket VLP and even higher than HA content for the H3N2 VLPs. M1 content was lower than HA and NA for both strains. NTA showed a polydispersity with a median particle size around 118 nm, close to the size of the virus [36]. The most abundant proteins were HA and NA (SDS-PAGE; Fig. 4). HA multimers and NA dimers were present in the VLP samples under non-reducing conditions. HA0 was not observed to cleave into HA1 and HA2 for A/Hong Kong/4801/2014 (H3N2) or B/Phuket/3073/2013. For A/California/07/09 (H1N1) however, HA (Fig. 2A) was partially cleaved into HA1 and HA2, without the addition of trypsin to the medium during VLP expression. HA cleavage is necessary only for viral re-infection. The HA from A/California/07/2009 (H1N1) is known to be less stable than that of other strains which could explain our observations [37]. Annotations were confirmed after band identification by MALDI-TOF/TOF mass spectrometry (data not shown). HA and NA bands increased their mobility after PNGase treatment, demonstrating that the two predominant viral surface antigens were glycosylated by N-linked oligosaccharides. Some minor bands were observed related to cellular proteins associated and incorporated into mammalian VLPs, as described by Wu and colleagues or recently by Venereo-Sanchez and colleagues [12,19]. HA, NA and M1 were estimated by densitometry to be around 90% percent pure for the two batches (supplementary material). Cryo-electron microscopy for the purified H3N2 and B/Phuket VLPs showed particle size of around 100 nm, decorated with spikes and with a lipid membrane resembling those observed for the sucrose gradient semi-purified VLPs in Fig. 2B (Fig. 2B and supplementary material).

3.4. Immunogenicity of VLPs

The immunogenicity of the influenza H3N2 and B/Phuket VLPs without addition of any adjuvant was evaluated in mice following a two-injection immunization schedule illustrated in Fig. 5A. HI titers $\geq$ 1:40, the threshold which reflects protection in humans, were obtained for all mice vaccinated with VLP vaccine at the dose of 1.2 μg of HA, and for 9/10 mice vaccinated with a 0.4 μg dose at day 42 (3 weeks after the second dose) against the two strains (Fig. 5B). The geometric means of HA titers were 435 and 260 for H3N2 and B/Phuket VLPs, respectively, at the 1.2 μg dose, and 279 and 197 at the 0.4 μg dose. The specific IgG ELISA titers were around 4 $\log_{10}$ EU for the two antigen doses and for the two strains, confirming the HI responses. NI titers were positive for all the animals.

Unexpectedly, NI titers obtained with the B/Phuket VLP were higher than those for the H3N2 VLPs. This might be a bias induced by the ELLA assay knowing that N2 VLPs had a lower activity with fetuin substrate compared to NA B/Phuket VLP. The means between the two doses were not statistically different for HI, IgG, and NI assays, but a globally lower HI response was observed with 0.4 μg of VLP than with 1.2 μg for both strains. For the B/Phuket VLPs, 0.13 μg was additionally tested in another experiment using the same immunization schedule and induced positive HI, NI and IgG responses (data not shown).

To complement the immunogenicity results obtained in mice, influenza H3N2 VLPs were assessed in an *in vitro* human assay termed the MIMIC® system (Fig. 6). Of note, we have previously demonstrated a strong correlation between HI and SA-HAI assay that is used in the MIMIC® system, with SA-HAI being more sensitive than the classical HI assay [35]. The analysis using the MIMIC®

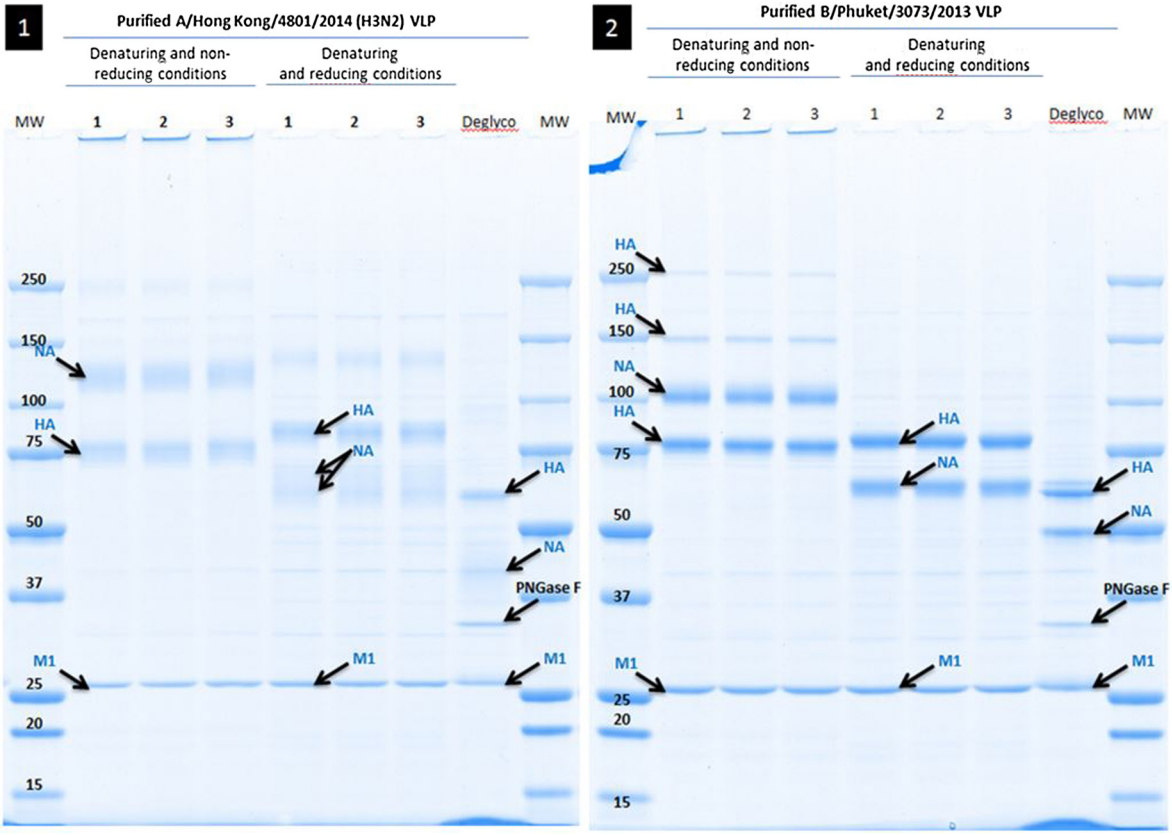

Fig. 4. VLP proteins were separated by SDS-PAGE and stained with Coomassie blue. (1) H3N2 VLP, (2) B/Phuket VLP.

system performed here was not sufficiently powered for us to be able to perform statistical analyses, but we were able to use the data to trend the response profiles and to confirm results obtained in animal experiments. The responses obtained for total IgG and SA-HAI readouts indicated that the H3N2 VLPs were immunogenic, and induced an *in vitro* immune response from human PBMC that was comparable to the inactivated H3N2 vaccine.

4. Discussion

In this study, we studied the feasibility to establish a platform to generate mammalian influenza VLPs as vaccine candidates by transient expression of three viral proteins HA, NA and M1.

We assessed three cell lines: CHO-K1, Vero and 293 T cells. CHO-K1 cells are extensively used to produce recombinant antibodies [38] and to produce new vaccine candidates [39]. Vero cells are used to produce vaccines such as polio, rabies or dengue vaccines [40,41]. 293 T cells are known for their susceptibility to transfection and are generally used by suppliers of transfection reagents or transfection equipment as a reference cell line for the high yield of heterologous protein expressed after transfection. Furthermore, 293 T cells were used by several research teams to produce VLPs [42–44].

That study showed that CHO cells produced VLPs with low density of HA and NA spikes on the surface. VLP production was poorly effective in Vero cells but VLPs produced in this cell line were very homogeneous with a high density of spikes on their surface. The poor VLP production yield in Vero cells is certainly related to the resistance of this cell line to transfection [23]. Hence, another transient or stable transfection protocol on micro-carriers or with suspension adapted Vero cells could be used to optimize yield. Of note, Wu and colleagues reported the production of VLPs from adherent Vero cells cultivated with serum by stable co-expression of four influenza structural proteins (HA, NA, M1 and M2) [12].

The 293 T cell line gave the best VLP yield and morphology. However, it is likely that 293 T cells would only be accepted by health authorities for vaccine production if the purification process could drastically reduce the cellular DNA content, as tumorigenicity issues have been associated with this cell line [45].

The M1 protein of A/California/07/2009 (H1N1), which has been reported to efficiently induce and complete budding at the plasma membrane by itself [21], was chosen for all the VLPs expressing the HA and NA from type A or B. In contrast, the M1 from the A/Puerto Rico/8/1934 (H1N1) (PR8) strain demonstrated poor efficiency in terms of VLP release from 293 cells [15]. For that reason, HIV-1 Gag is often preferred to influenza M1. The expression of HA after HA-NA-Gag co-expression has been shown to be 7-fold higher than with a HA-NA-PR8/M1 combination [15]. The highest yield of HA in our study, monitored by SRID after purification was obtained with H3N2 VLPs (1.32 mg per liter of culture); this yield being far higher than the one related by Venereo-Sanchez (138 μg per liter) using 293 cells stably expressing the HA and NA from the PR8 strain with the HIV-1 Gag protein [15].

However, we observed considerable differences in VLP yields between the 4 influenza strains tested. H3N2 and B/Phuket VLPs presented high yields and could be purified easily. H1N1 and B/Brisbane VLPs showed low yields and purification was not successful. VLP budding and release occur through a process that is similar to influenza virion budding. In particular, the role of NA was highlighted in the budding of the virus and VLPs [46]. Therefore, the differences in VLP yields observed with the various viral strains could be attributed to the NAs from H3N2 and B/Phuket being more active than the NAs from H1N1 and B/Brisbane. Moreover, HA and NA present antagonistic activities, with NA cleaving

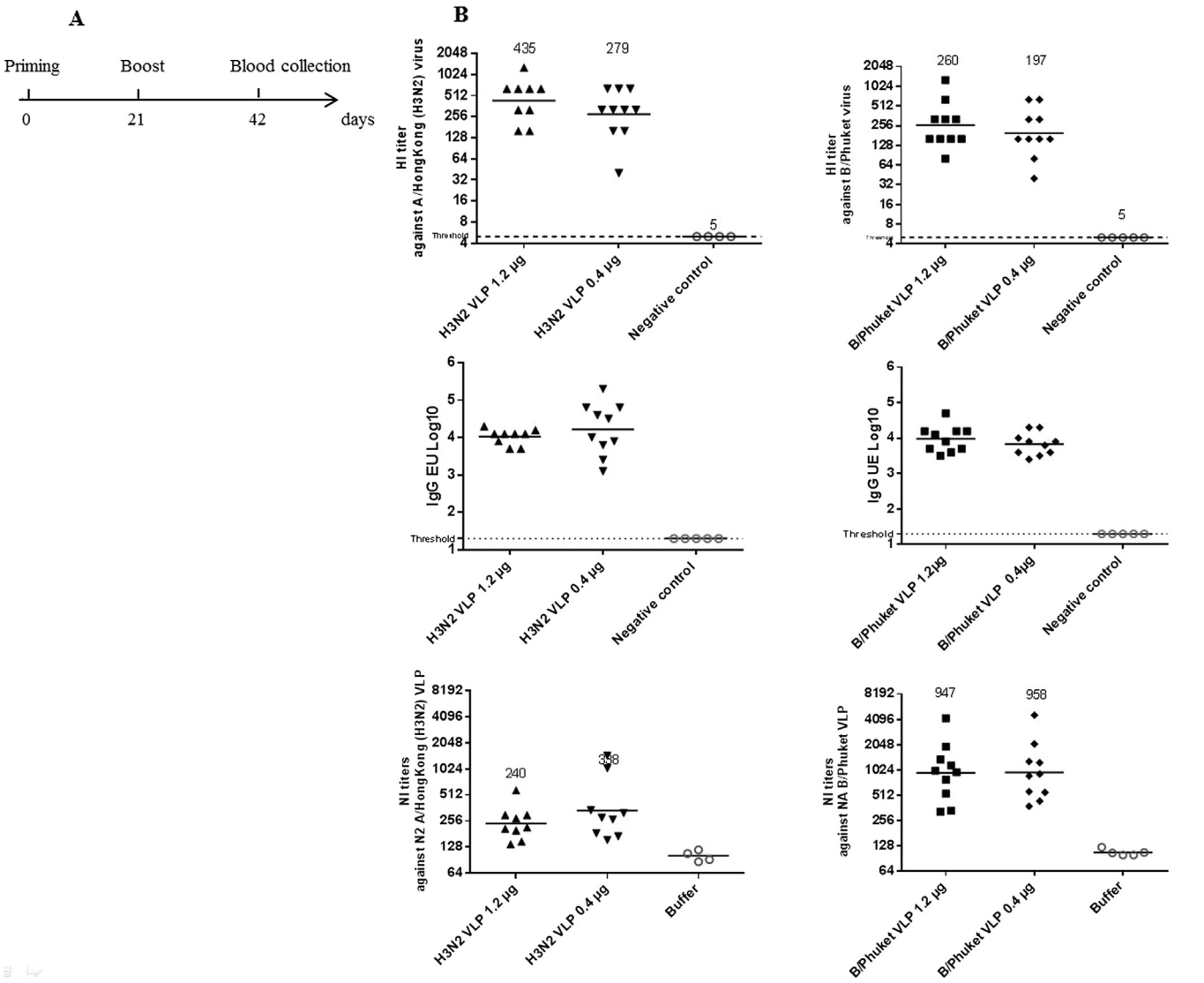

Fig. 5. Immunogenicity of influenza VLPs in mice. (A) Immunization design, (B) HI, IgG and NI titers at day 42 in sera. Each individual dot represents the value from a single mouse, and the horizontal line represents the geometric mean values. HI titer of 5 and ELISA titer of 1.3 log10 was the threshold. There was no significant difference between means of the 2 doses 1.2 and 0.4 µg for HI, IgG and NI assays using a Student *t*-test.

the sialic acid residues and HA attaching to them. Hence one cannot exclude that both proteins were probably implicated in the mechanism triggering the observed yields for the 4 strains.

In this study, an efficient VLP purification process was developed yielding a purity superior to 90% for the two batches produced. Three viral protein bands, corresponding to HA, NA and M1 were clearly visible on SDS-PAGE gel, HA and NA proteins being N-glycosylated. Impurities, most likely host cell proteins were observed on the SDS-PAGE gel as minor bands. This was expected as influenza VLPs are released after budding, as are influenza viruses, resulting in the acquisition of an envelope derived from host cells. In previous studies, 36 host-encoded proteins were detected in influenza virus particles propagated in MDCK cells [47]; the majority of them were also found in influenza VLPs produced in Vero cells [12]. In our study, the purified VLP batches contained more than 50 ng/mL of residual host cell DNA. The benzonase treatments eliminated more than 97% of DNA. However, the limit for the residual host cell DNA must be $\leq$ 100 pg per dose for parenteral administration and the DNA fragments should be reduced to below the size of a functional gene (assumed to be about 200 base pairs) [48]. Thus, further optimization of the purification process would be needed.

Under cryo-TEM, the purified VLPs closely resembled influenza virus in size, particle morphology, and fine structure of the surface spikes. The viral proteins, HA, NA, and M1, had approximately equivalent concentrations, probably because all genes are governed by the same promoter. Equal proportions of HA and NA molecules were found on these VLPs, which could result in enhanced immunity against NA compared to current influenza vaccines. Both glycoproteins were functional, HA (HAU) and NA (MUNANA) activities being very high in the two purified batches. Indeed, HA activity observed in this study was greater than that obtained by Venereo-Sanchez and Thompson [15,49]. Unfortunately, NA activity is rarely measured in the literature relating to influenza VLP production.

The immunogenicity studies using the influenza A and B VLPs demonstrated that VLPs induced high humoral responses in mice, with functional antibodies against HA, and against NA. In line with previous human studies [50], HI titers against the B strain were lower compared to A/H3N2 strains. It is important to note that in this study, we set up a new ELLA assay using VLPs as reagents, containing only NA (N2 from A/Hong Kong and NA from B/Phuket) and M1 without HA. The source of NA is an important consideration when performing this assay. Sera from vaccinated animals contain

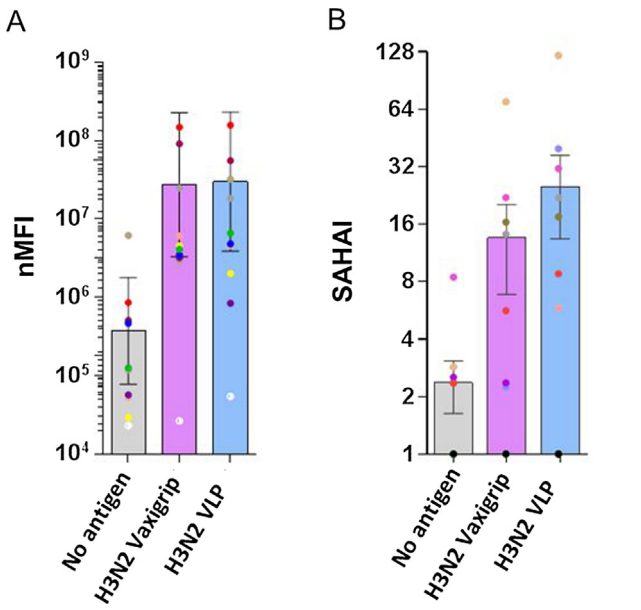

Fig. 6. Immunogenicity of influenza VLPs in MIMIC® model. Bars represent geometric mean with 95%CI (n = 10 donors), with each dot representing one donor. (A) Specific IgG responses against A/Hong Kong (H3N2) strain obtained upon MIMIC® *in vitro* vaccination with 10 ng of each vaccine, measured using Antibody Forensics and represented as Log normalized Median Fluorescence Intensity (nMFI) ; (B) Specific SA-HAI titers generated against A/Hong Kong (H3N2) strain obtained upon MIMIC® *in vitro* vaccination with 10 ng of each vaccine. SA-HAI lower limit of quantitation equals 2.

antibodies directed against HA and against NA. These anti-HA antibodies can neutralize the virus and create steric hindrance between NA and the assay substrate [51]. This could lead to an overestimation of NI titers.

One recognized significant shortcoming of animal models is their inability to accurately predict immunogenicity in humans, especially for influenza vaccine [52]. *In vitro* human models, such as the MIMIC® system, can be used to complement animal models for predicting vaccine efficacy. Recently, this system was used to study age-associated changes in immunological responses after influenza vaccination [34]. This system might be better suited than mice to evaluate human immunity to influenza since people can have multiple immunological exposures to influenza over their lifetimes, whereas laboratory mice are naïve to influenza. However, the system demonstrates greater heterogeneity in terms of response profiles due to the variability of the influenza immune status of human donors. In our study, the two analyses performed (IgG by antibody forensic and SA-HAI) using this system confirmed the immunogenicity of the VLPs as observed in the mice. Furthermore, the H3N2 VLP candidate was found to be as immunogenic as the H3N2 Vaxigrip monovalent. Further development of this influenza VLP vaccine could include ferret protection studies to confirm its potency as a vaccine before proceeding to clinical development.

To conclude, in the present work we developed a flexible VLP platform using 293 T cells. After purification and extensive characterization through powerful technologies such as mass spectrometry and cryo-EM, the resulting VLP were shown to be very immunogenic *in vivo* in mice without adjuvant and *in vitro* in the MIMIC® human system.

Declaration of Competing Interest

The authors declare the following financial interests/personal relationships which may be considered as potential competing interests: Sophie Buffin; Isabelle Peubez; Fabienne Barrière; Marie-Claire Nicolaï; Tenekua Tapia; Vipra Dhir; Eric Forma; Nicolas Sève; Isabelle Legastelois are all employees of Sanofi Pasteur. This study has been funded by Sanofi Pasteur.

Acknowledgments

We would like to thank Cornelia Alvarez, internship on this project, Christophe Chevalard for the bioreactor culture development, Stéphane Guichard and Séverine Nury for the purification process development. We would like to acknowledge Julien Burlaud-Gaillard (IBiSA, University of Tours), Marion Decossas (CBMN, UMR 5248, University of Bordeaux), Aurélie Deliot and Sergio Marco for electron microscopy analysis, Damien Soulet for nanoparticle tracking analysis, Catherine Manin for her expertise in mass spectrometry and Corinne Lyonnais for her technical assistance for SRID assay. We also thank the Animal Core Facility for their technical assistance, Marie-Clotilde Bernard, Sylvie Commandeur for their expertise in immunology. We would like to acknowledge Fabien Barbirato, Philippe-Alexandre Gilbert and Jean Haensler for their review of the manuscript.

Appendix A. Supplementary material

Supplementary data to this article can be found online at https://doi.org/10.1016/j.vaccine.2019.09.057.

References

[1] Getie-Kebtie M, Sultana I, Eichelberger M, Alterman M. Label-free mass spectrometry-based quantification of hemagglutinin and neuraminidase in influenza virus preparations and vaccines. Influenza Other Respir Viruses 2013;7:521–30.
[2] Cohen M et al. Influenza A penetrates host mucus by cleaving sialic acids with neuraminidase. Virol J 2013;10:321.
[3] Gomez Lorenzo MM, Fenton MJ. Immunobiology of influenza vaccines. Chest 2013;143:502–10.
[4] WHO. WHO | Influenza (Seasonal). WHO (2016). Available at: http://www.who.int/mediacentre/factsheets/fs211/en/ [Accessed: 24th April 2017].
[5] Krammer F et al. NAction! How can neuraminidase-based immunity contribute to better influenza virus Vaccines? mBio 2018;9.
[6] Pica N, Palese P. Toward a universal influenza virus vaccine: prospects and challenges. Annu Rev Med 2013;64:189–202.
[7] Manini I et al. Flucelvax (Optaflu) for seasonal influenza. Expert Rev Vaccines 2015;14:789–804.
[8] Dunkle LM et al. Efficacy of recombinant influenza vaccine in adults 50 years of age or older. N Engl J Med 2017;376:2427–36.
[9] López-Macías C et al. Safety and immunogenicity of a virus-like particle pandemic influenza A (H1N1) 2009 vaccine in a blinded, randomized, placebo-controlled trial of adults in Mexico. Vaccine 2011;29:7826–34.
[10] Mohsen MO, Zha L, Cabral-Miranda G, Bachmann MF. Major findings and recent advances in virus–like particle (VLP)-based vaccines. Semin Immunol 2017;34:123–32.
[11] Hu C-MJ et al. Multi-antigen avian influenza a (H7N9) virus-like particles: particulate characterizations and immunogenicity evaluation in murine and avian models. BMC Biotechnol 2017;17.
[12] Wu C-Y et al. Mammalian expression of virus-like particles for advanced mimicry of authentic influenza virus. PLoS One 2010;5.
[13] Pillet S et al. A plant-derived quadrivalent virus like particle influenza vaccine induces cross-reactive antibody and T cell response in healthy adults. Clin Immunol 2016;168:72–87.
[14] Tretyakova I et al. Preparation of quadri-subtype influenza virus-like particles using bovine immunodeficiency virus gag protein. Virology 2016;487:163–71.
[15] Venereo-Sanchez A et al. Hemagglutinin and neuraminidase containing virus-like particles produced in HEK-293 suspension culture: An effective influenza vaccine candidate. Vaccine 2016;34(29):3371–80.
[16] Maegawa K et al. Overexpression of a virus-like particle influenza vaccine in Eri silkworm pupae, using Autographa californica nuclear polyhedrosis virus and host-range expansion. Arch Virol 2018;163:2787–97.
[17] Cervera L, Kamen AA. Large-Scale Transient Transfection of Suspension Mammalian Cells for VLP Production. In: Picanço-Castro V, Swiech K, editors. Recombinant glycoprotein production, vol. 1674. New York: Springer; 2018. p. 117–27.
[18] Venereo-Sanchez A et al. Process intensification for high yield production of influenza H1N1 Gag virus-like particles using an inducible HEK-293 stable cell line. Vaccine 2017;35:4220–8.

[19] Venereo-Sánchez A et al. Characterization of influenza H1N1 Gag virus-like particles and extracellular vesicles co-produced in HEK-293SF. Vaccine 2019;37(47):7100–7.
[20] Gutiérrez-Granados S, Cervera L, Kamen AA, Gòdia F. Advancements in mammalian cell transient gene expression (TGE) technology for accelerated production of biologics. Crit Rev Biotechnol 2018;38:918–40.
[21] Bialas KM, Desmet EA, Takimoto T. Specific Residues in the 2009 H1N1 swine-origin influenza matrix protein influence virion morphology and efficiency of viral spread in vitro. PLoS One 2012;7.
[22] Cheng EH-Y et al. A Bcl-2 homolog encoded by Kaposi sarcoma-associated virus, human herpesvirus 8, inhibits apoptosis but does not heterodimerize with Bax or Bak. Proc Natl Acad Sci USA 1997;94:690–4.
[23] Medina J et al. Vero/CHOK1, a novel mixture of cell lines that is optimal for the rescue of influenza A vaccine seeds. J Virol Methods 2014;196:25–31.
[24] Stöhr K, Bucher D, Colgate T, Wood J. Influenza virus surveillance, vaccine strain selection, and manufacture. Influenza Virus 2012:147–62. https://doi.org/10.1007/978-1-61779-621-0_9.
[25] Gerber SA, Rush J, Stemman O, Kirschner MW, Gygi SP. Absolute quantification of proteins and phosphoproteins from cell lysates by tandem MS. Proc Natl Acad Sci 2003;100:6940–5.
[26] Williams TL, Pirkle JL, Barr JR. Simultaneous quantification of hemagglutinin and neuraminidase of influenza virus using isotope dilution mass spectrometry. Vaccine 2012;30:2475–82.
[27] MacLean B et al. Skyline: an open source document editor for creating and analyzing targeted proteomics experiments. Bioinformatics 2010;26:966–8.
[28] E56 Committee. Guide for measurement of particle size distribution of nanomaterials in suspension by nanoparticle tracking analysis (NTA). ASTM International. https://doi.org/10.1520/E2834-12R18.
[29] Burlaud-Gaillard J et al. Correlative scanning-transmission electron microscopy reveals that a chimeric Flavivirus Is Released as individual particles in secretory vesicles. PLoS One 2014;9:e93573.
[30] Pion C et al. Characterization and immunogenicity in mice of recombinant influenza haemagglutinins produced in Leishmania tarentolae. Vaccine 2014;32:5570–6.
[31] Ananthanarayan R, Paniker CKJ. Non-specific inhibitors of influenza viruses in normal sera. Bull World Health Organ 1960;22:409–19.
[32] Couzens L et al. An optimized enzyme-linked lectin assay to measure influenza A virus neuraminidase inhibition antibody titers in human sera. J Virol Methods 2014;210:7–14.
[33] Schanen BC, Drake DR. A novel approach for the generation of human dendritic cells from blood monocytes in the absence of exogenous factors. J Immunol Methods 2008;335:53–64.
[34] Dauner A et al. The in vitro MIMIC® platform reflects age-associated changes in immunological responses after influenza vaccination. Vaccine 2017;35:5487–94.
[35] Drake DR et al. *In Vitro* biomimetic model of the human immune system for predictive vaccine assessments. Disruptive Sci Technol 2012;1:28–40.
[36] Kramberger P, Ciringer M, Štrancar A, Peterka M. Evaluation of nanoparticle tracking analysis for total virus particle determination. Virol J 2012;9:265.
[37] Cotter CR, Jin H, Chen Z. A Single amino acid in the stalk region of the h1n1pdm influenza virus HA protein affects viral fusion. Stability and Infectivity. PLOS Pathog 2014;10:e1003831.
[38] Li F, Vijayasankaran N, Shen A, Yijuan Kiss R, Amanullah A. Cell culture processes for monoclonal antibody production. mAbs 2010;2:466–77.
[39] Hofmann I et al. Expression of the human cytomegalovirus pentamer complex for vaccine use in a CHO system. Biotechnol Bioeng 2015;112:2505–15.
[40] Barrett PN, Mundt W, Kistner O, Howard MK. Vero cell platform in vaccine production: moving towards cell culture-based viral vaccines. Expert Rev Vaccines 2009;8:607–18.
[41] Ehrlich HJ et al. Clinical development of a Vero cell culture-derived seasonal influenza vaccine. Vaccine 2012;30:4377–86.
[42] Cervera L et al. Generation of HIV-1 Gag VLPs by transient transfection of HEK 293 suspension cell cultures using an optimized animal-derived component free medium. J Biotechnol 2013;166:152–65.
[43] Garg H, Sedano M, Plata G, Punke EB, Joshi A. Development of virus-like-particle vaccine and reporter assay for Zika virus. J Virol 2017;91.
[44] Lai JCC et al. Formation of virus-like particles from human cell lines exclusively expressing influenza neuraminidase. J Gen Virol 2010;91:2322–30.
[45] Stepanenko AA, Dmitrenko VV. HEK293 in cell biology and cancer research: phenotype, karyotype, tumorigenicity, and stress-induced genome-phenotype evolution. Gene 2015;569:182–90.
[46] Chlanda P et al. Structural analysis of the roles of influenza A virus membrane-associated proteins in assembly and morphology. J. Virol 2015;89:8957–66.
[47] Shaw ML, Stone KL, Colangelo CM, Gulcicek EE, Palese P. Cellular proteins in influenza virus particles. PLoS Pathog 2008;4:e1000085.
[48] Vernay O et al. Comparative analysis of the performance of residual host-cell DNA assays for viral vaccines produced in Vero cells. J Virol Methods 2019. https://doi.org/10.1016/j.jviromet.2019.01.001.
[49] Thompson CM et al. Critical assessment of influenza VLP production in Sf9 and HEK293 expression systems. BMC Biotechnol 2015;15.
[50] Couch RB et al. Randomized comparative study of the serum antihemagglutinin and antineuraminidase antibody responses to six licensed trivalent influenza vaccines. Vaccine 2012;31:190–5.
[51] Rajendran M et al. Analysis of anti-influenza virus neuraminidase antibodies in children, adults, and the elderly by ELISA and enzyme inhibition: evidence for original antigenic. Sin mBio 2017;8:e02281–e2316.
[52] Bodewes R, Rimmelzwaan GF, Osterhaus AD. Animal models for the preclinical evaluation of candidate influenza vaccines. Expert Rev Vaccines 2010;9:59–72.